UNIDIRECTIONAL PERIODIC FLOW ABOUT CIRCULAR CYLINDERS

Richard Doyle Greenamyer

NAVAL POSTGRADUATE SCHOOL
Monterey, California

THESIS

UNIDIRECTIONAL PERIODIC FLOW
ABOUT CIRCULAR CYLINDERS

by

Richard Doyle Greenamyer

Thesis Advisor: T. Sarpkaya

June 1973

Unidirectional Periodic Flow About Circular Cylinders

by

Richard Doyle Greenamyer
Lieutenant, United States Navy
A.B., University of North Carolina at Chapel Hill, 1966

Submitted in partial fulfillment of the
requirements for the degree of

MASTER OF SCIENCE IN MECHANICAL ENGINEERING

from the

NAVAL POSTGRADUATE SCHOOL
June 1973

ABSTRACT

The instantaneous force acting on a circular cylinder immersed in a unidirectional periodic flow characterized by $U = \overline{V} + V_A \sin 2\pi ft$ was investigated. The total force was divided into three components consisting of a steady-state drag; an oscillating drag which is a function of the frequency parameter $\lambda = fd/\overline{V}$; and an inertial force which is also a function of the frequency parameter. The three resistance coefficients associated with the force components, $C_D(0)$, $C_D(\lambda)$, and $C_M(\lambda)$ were calculated.

It was found that the resistance coefficients are not materially affected by the free-stream oscillations whenever the frequency of the oscillation is lower than the natural frequency of the vortex shedding. However, when λ approaches the Strouhal frequency of vortex shedding, the inertia coefficient C_M is significantly reduced, and likewise when λ approaches the value of twice the Strouhal number, $C_D(\lambda)$ is markedly reduced. In regions below this range, the inertial force becomes negligible and the total resistance could be represented accurately by the coefficients $C_D(0)$ and $C_D(\lambda)$ with C_M fixed at its theoretical unseparated-flow value, 2.0.

TABLE OF CONTENTS

LIST OF FIGURES

NOMENCLATURE

Symbol	
A	effective cylinder flow-blockage area ($A = d\ell$)
a	instantaneous acceleration
A_o	cylinder cross-sectional area ($A_o = \pi d^2/4$)
A_{TS}	cross-sectional area of test section ($A_{TS} = h\ell$)
C_D	steady state drag coefficient
$C_D(0)$	coefficient for steady state portion of drag
$C_D(\lambda)$	coefficient for oscillating portion of drag
$C_M(\lambda)$	coefficient for inertia force
d	diameter of test cylinder
e	tunnel correction factor
F	instantaneous total force acting on the test cylinder
f	frequency of oscillation
F_D	drag forces acting on the test cylinder
F_I	inertia forces acting on the test cylinder
h	height of tunnel test section
K_1	constant ($K_1 = \frac{1}{2}\rho\bar{V}^2A$)
K_2	constant ($K_2 = \bar{V}V_A A\rho$)
K_3	constant ($K_3 = \frac{1}{2}V_A{}^2 A\rho$)
K_4	constant ($K_4 = 2\pi f\rho A_o \ell V_A$)
ℓ	width of tunnel test section; test cylinder length
n	frequency of vortex shedding
P	pressure
p	height of dynamic pressure curve at t = T/4

q	measured velocity
R	test cylinder radius
r	height of dynamic pressure curve at $t = 3T/4$
Re	Reynolds number ($Re = Ud/\nu$)
$\overline{Re}$	Reynolds number ($\overline{Re} = \overline{V}d/\nu$)
St	Strouhal number ($St = nd/\overline{V}$)
T	period of oscillation
t	time
U	instantaneous velocity ($U = \overline{V} + V_A \sin 2\pi ft$)
V	free stream velocity
V_A	amplitude of velocity oscillation
$\overline{V}$	average velocity
X	horizontal distance between pressure taps 1 and 3
Y	horizontal distance between pressure tap 3 and center of test cylinder
λ	normalized frequency of oscillation ($\lambda = fd/\overline{V}$)
ν	fluid kinematic viscosity
ρ	fluid density

I. INTRODUCTION

A. EXPERIMENTAL JUSTIFICATION

The subject of forces acting on bluff bodies immersed in time-dependent flows has been and will continue to be of interest to fluid dynamicists, aerodynamicists, and practicing engineers for the special reason that in nature neither the body nor the fluid which surrounds the body is ever in a state of steady motion. Even the flow behind a bluff body moving steadily through a fluid is accompanied by large scale unsteadiness. Thus, any type of unsteadiness of the ambient flow and/or the motion of the body introduces additional changes in the characteristics of the flow and its analysis.

The drag and inertial forces are interdependent as well as time dependent, and the resistance coefficients obtained in unseparated flows are not applicable to separated cases. Although indirect, the role of viscosity is paramount in that its consequences are separation, vortex formation and shedding, and resultant alternations in the virtual mass. It is thus clear that it is necessary to determine the relationships between various resistance components in terms of the unsteadiness of the ambient flow and/or body motion, geometry of the body, the degree of upstream turbulence, past history of the flow, etc. [Ref. 1].

However, the understanding of the behavior of time-dependent flows about bluff bodies may be advanced only by considering the relatively more manageable cases and gradually integrating the information so obtained. This led to the present experimental investigation of the unidirectional periodic flow about circular cylinders.

B. SURVEY OF THE PREVIOUS INVESTIGATIONS[1]

A review of some of the previous investigations on time-dependent flows may best be presented by dividing the motions under consideration into various but admittedly arbitrary categories.

1. Theoretical Analysis of Unseparated Time-Dependent Laminar Flows

The study of the theory of separation-free time-dependent laminar flows has enjoyed particular attention, partly due to its practical significance and partly due to its relative mathematical simplicity. Surveys by Stewartson [Ref. 2], Stuart [Ref. 3], and Rott [Ref. 4] reflect the current level of understanding.

The unseparated class of unsteady flows, most of which results from the unidirectional or periodic acceleration of bodies in an infinite or bounded fluid medium, gives rise to an induced mass which must be added to the real mass of the body. In general, the virtual inertia tensor depends

---

[1]This section has been reproduced here, by permission, from an unpublished report by Prof. T. Sarpkaya.

on the shape of the body, the nature of the fluid medium, the orientation of the moving object with respect to the direction of motion, and the depth of relative submergence from a free surface and/or solid boundary.

The effects of viscosity and separation on added mass or the dependence of added mass of a given body on the characteristics of the time-dependent separated flow cannot yet be theoretically evaluated nor can it be experimentally separated from the total resistance experienced by the body.

2. Small Amplitude Vibration of Bodies in a Liquid Otherwise at Rest and the Initial Instants of Acceleration of Bodies from a State of Uniform Velocity

Vibratory motion has often been used [Refs. 5-8] as one of the experimental means to determine the virtual mass coefficients. The technique has been restricted to amplitudes of motion which are so small that either separation does not occur or the characteristics of separation do not change due to the imposed, high-frequency vibration. Thus, the results obtained are not applicable to occurrences in which the duration of unsteady flow in one direction is long enough for separation to occur.

It is not necessary that the body be initially at rest to determine the added mass provided that one starts with a steady ambient flow about the body or with the body moving at constant velocity in a fluid otherwise at rest. Hamilton and Lindell [Ref. 9] have shown that the added-mass coefficient of a sphere determined by imposing a uniform

acceleration onto its steady state motion is equal to its theoretically determined value as well as to its experimentally determined value obtained by small-amplitude, high-frequency oscillations.

Rayleigh [Ref. 10] has shown that if the acceleration continues, i.e. $V = \bar{V} + kt^m$, both the drag and the added-mass coefficients change with time.

The foregoing arguments suggest that the force exerted by the fluid on a body immersed in a time-dependent flow might be expressed as

$$F = \underbrace{\tfrac{1}{2}C_D\rho A|\bar{V}|\bar{V} + C_M m_f \, dV/dt}_{\text{drag and inertia forces}} + \text{history-dependent} \qquad (1)$$

in which A is the projected area of the body and m_f the mass of the fluid displaced by the body. The drag coefficient C_D is to be taken equal to the quasi-steady state resistance coefficient and C_M to be taken equal to that measured or calculated from the potential theory when the value of the history-dependent force is zero [Ref. 9].

3. Bodies Subjected to Large Amplitude Harmonic Oscillations in a Fluid Otherwise at Rest

A number of significant studies [Refs. 11-15] were made to determine the forces acting on bluff bodies undergoing harmonic, large-amplitude oscillations in a liquid otherwise at rest.

Odar and Hamilton [Ref. 11] measured the force acting on a sphere subjected to harmonic oscillations and proposed a force equation comprised of three parts: a steady drag component where the drag coefficient is the well-established coefficient for steady translation of a sphere; an inertial component whose coefficient is determined experimentally as a function of V^2/ad (a: acceleration; d: diameter of sphere); and a history-dependent component whose coefficient also is a function of V^2/ad.

4. Bodies Subjected to Wave Motion with Zero Mean Velocity

Considerable work [Refs. 16-21] has been done on this type of time-dependent flow in an attempt to predict the wave forces on piles and other submerged structures. In general, the total force acting on the body is assumed to be composed of a velocity-dependent and an acceleration-dependent force. The resulting equation, known as the Morison equation [Ref. 16], is given by

$$F = \tfrac{1}{2}C_D\rho A|\bar{V}|\bar{V} + C_M m_f \, dV/dt \qquad (2)$$

where $C_M = 1 + C$, C being the added mass coefficient. Experiments show that C_D and C_M depend on time and show considerable scatter about their assumed mean values [Refs. 17, 20] over a cycle.

5. Bodies Subjected to Unidirectional Acceleration in a Fluid Otherwise at Rest or Unidirectional Unsteady Flow About Bodies Held at Rest

Substantial effort has been made to determine the components of force acting on a body accelerating unidirectionally in a fluid otherwise at rest. Iverson and Balent [Ref. 22] and Keim [Ref. 23] towed spheres, disks, and cylinders in unsteady motion through still water. It was concluded that the total instantaneous force on these objects could be described by a single coefficient of the form $C = 2F/\rho AV^2$ and that this coefficient was a function only of a so-called acceleration modulus, ad/V^2. Keim, however, detected an apparent Reynolds number effect for cylinders.

Laird et. al. [Ref. 24] measured the forces acting on accelerating cylinders and found strong evidence of deviation of the drag coefficient from the accepted values for uniform motion. They further found that the acceleration modulus did not correlate the resistance coefficient near boundary-layer transition.

Sarpkaya and Garrison [Ref. 22] working with unidirectional flow with constant acceleration about cylinders and plates have found that both C_D and C_M depend on the history of motion, that the Morison equation (Eqn. 2) is valid only for flows with constant acceleration, and that the acceleration modulus can correlate the data only if the acceleration is kept constant.

6. Forced or Self-Induced Transverse Oscillations of a Body in a Fluid in Steady Motion

Experiments have been directed to the effects that attend the oscillations of a body in the plane of the lift force. This type of interaction becomes particularly important when the oscillation of the structure is the necessary condition for the generation of the exciting forces. The most pertinent information from these experiments is that the lift and drag forces act on the oscillating cylinder at the vortex shedding frequency and twice the shedding frequency, respectively, provided that the driving frequency on the cylinder is appreciably different from the shedding frequency. When the forcing frequency of the cylinder approaches the shedding frequency, the natural shedding frequency is lost and it "locks-in" to the forcing frequency. This synchronization persists over a range of frequencies which may be termed the "range of synchronization" [Ref. 26].

7. Unidirectional Oscillatory Flow About Bodies at Rest and Steady Uniform Flow About Bodies Subjected to Streamwise Oscillations

Relatively few studies have been conducted in this category. Chen and Ballengee [Ref. 27] examined the vortex shedding from circular cylinders in an oscillating free stream. Their results suggested that "in an oscillatory freestream of 3 HZ and Reynolds number up to 40,000, the vortex shedding from a circular cylinder responds instantaneously to the freestream variations" and that "the instantaneous Strouhal number stays sensibly constant at 0.2 ± 0.01."

Hatfield and Morkovin [Ref. 28] studied the effect of an oscillating free stream on the unsteady pressure on a circular cylinder. They have found that there is no significant coupling between the small-amplitude free-stream oscillations and the vortex shedding. Their results would suggest that the drag coefficient associated with the mean flow would essentially remain constant at its steady state value. On the other hand, Mercier [Ref. 29] who subjected cylinders to large streamwise oscillations found that the average drag coefficient significantly increases with fd/V and that the rate of increase depends on the amplitude to diameter ratio. Combined, these results would suggest that the degree of coupling between the frequency of oscillation and the vortex-shedding frequency and hence the forces acting on the body strongly depend on the amplitude of oscillation.

Davenport [Ref. 30] subjected bluff bodies to small amplitude oscillations in a water flume and evaluated the drag and inertia coefficients through the measurement of the rate of damping of the amplitude of oscillations of the bodies, i.e. without measuring the forces acting on the bodies. Using the frequency parameter $fd/\overline{V}$ to correlate the data, he found large variations in C_D and C_M.

C. SCOPE OF THE PRESENT STUDY

The present investigation is limited to an experimental determination of the instantaneous forces acting on a circular cylinder immersed in a unidirectional periodic

flow characterized by

$$U = \bar{V} + V_A \sin 2\pi ft. \qquad (3)$$

Its theoretical aspects are structured along the lines of the unpublished work by Sarpkaya [Ref. 31] conducted at Aerodynamische Versuchsanstalt-Göttingen with respect to the supposition that the instantaneous force acting on an object immersed in a periodic flow strongly depends on the parameter $fd/\bar{V}$ and to varying degrees on $\bar{V}d/\nu$ and $V_A/\bar{V}$ where f is the frequency of oscillation and d the cylinder diameter.

The range of these parameters during the experimental work was:

$$0.0001 < fd/\bar{V} < 0.05$$
$$11{,}000 < \bar{V}d/\nu < 63{,}000$$
$$0.085 < V_A/\bar{V} < 0.69$$

As presented in Section IV, the parameter $fd/\bar{V}$ is extended to a value of 1.5 using the data of others.

II. APPARATUS AND PROCEDURE

A. APPARATUS

1. Water Tunnel and Oscillating Mechanism

The experiments were conducted in a 500-gallon-capacity, recirculating-type water tunnel as shown in Figure 1. Water was circulated by a low-rpm, high-capacity, centrifugal pump which was capable of providing test-section mean velocities of 2-25 feet per second. The test section consisted of a rectangular conduit 4 inches wide, 8 inches high, and 16 inches long.

Periodic variations in water velocity were provided by a rotating butterfly valve driven by a variable speed motor capable of a range of 0-40 rpm (Fig. 2). The magnitude of the velocity fluctuations was dependent upon the loss in effective head through the valve. As this is partially a function of the valve-to-conduit area ratio [Refs. 35,36], an access plate was placed on the tunnel in order to change the effective valve area by adding concentric rings to the valve perimeter without removing or changing the valve body.

Associated with the tunnel is a 15-gallon head tank located 12 feet above the test section centerline.

2. Test Specimens

The test specimens consisted of polished aluminum cylinders placed across the width of the test section perpendicular to the direction of flow (Fig. 3). A small bore

A	AIR VENT	SC	SPEED CONTROL
BV	BUTTERFLY VALVE	TS	TEST SECTION
CP	CENTRIFUGAL PUMP	1	TO 15 GALLON HEAD TANK
M	MOTOR	2	TO DRAINAGE AND FILL LINE
N	NOZZLE SECTION		

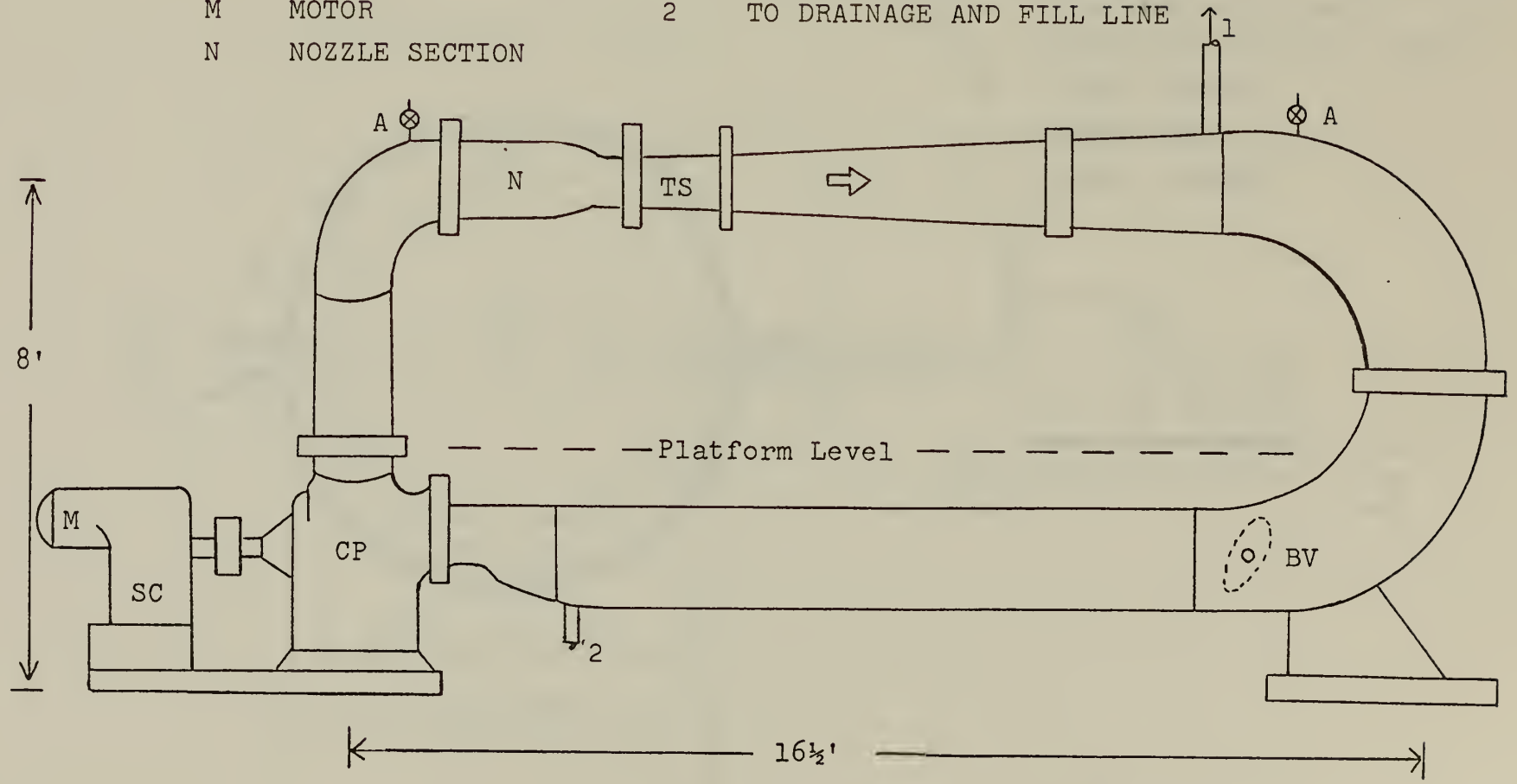

Figure 1: WATER TUNNEL

AP ACCESS PLATE
CR CONCENTRIC RINGS
D DIAMETER OF VALVE (including concentric rings)
M MOTOR AND REDUCTION GEAR
WT WATER TUNNEL
VB VALVE BODY
SC SPEED CONTROL

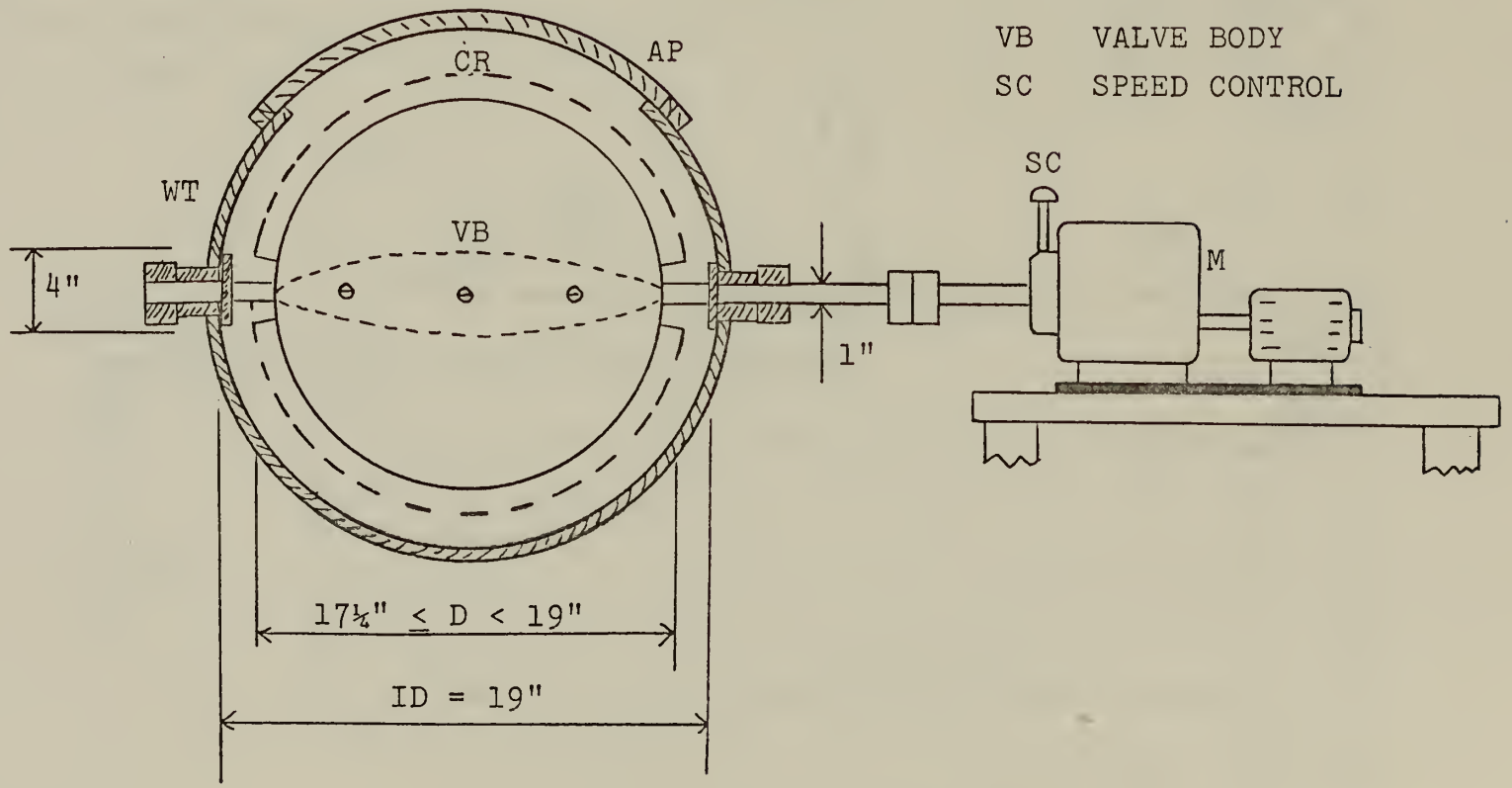

Figure 2: BUTTERFLY VALVE

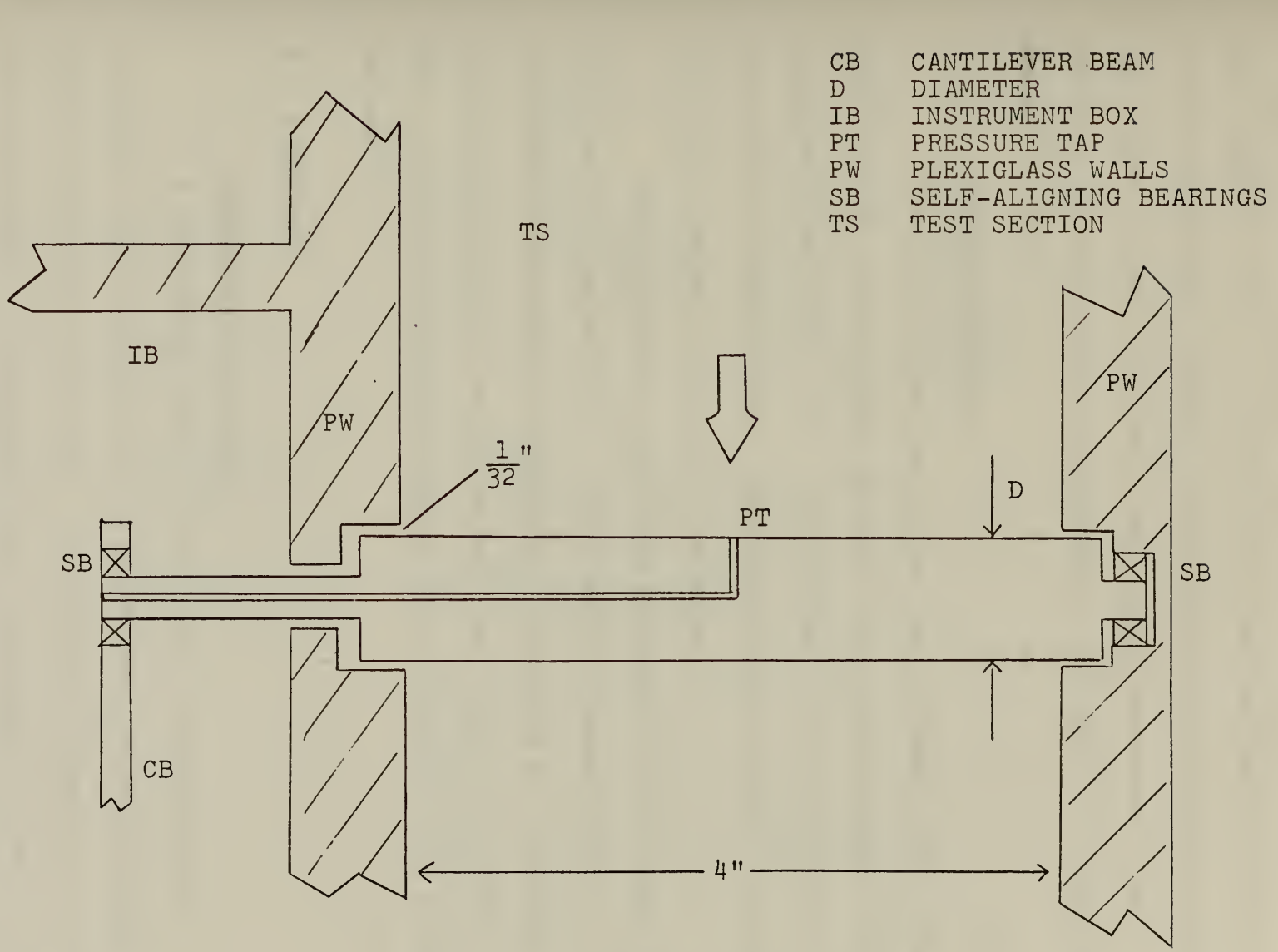

Figure 3: TEST SPECIMEN

hole drilled radially from the cylinder surface at the mid-section served as the total pressure tap. The test cylinder was mounted with one end held by a self-aligning bearing fit in one plexiglass window, with the other end passing through the other window to a cantilever beam force-measurement system. Two cylinders of diameters 0.75 and 1.0 inches were used.

3. Instrumentation

The total force acting on the cylinder within the test section was measured directly by a strain-gage fitted cantilever beam (Fig. 4). The bridge circuit consisted of four active strain gages, with the output signal being fed to a dual-channel strip chart recorder.

Three pressure taps were utilized for velocity and acceleration calculations. Two variable-sensitivity, differential-pressure transducers connected to two dual-channel strip chart recorders were used for this purpose. Each transducer/recorder system was calibrated with a water-manometer.

B. PROCEDURE

1. Measurement of Force

A continuous trace of the total, instantaneous force acting on the cylinder was obtained from the strain-gage fitted cantilever beam (Fig. 4) which was wired to a strip chart recorder. This system was calibrated by static loading of the cylinder. Three different cantilever beams were used

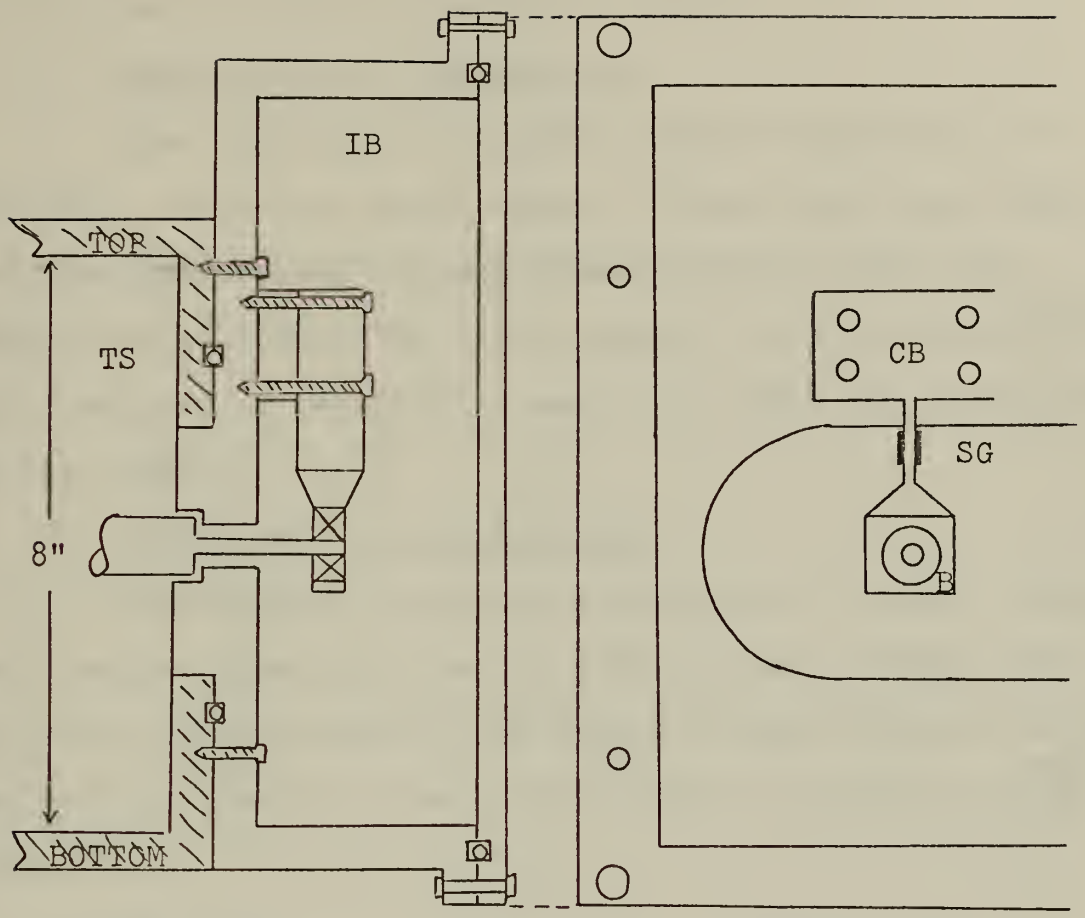

B	SELF-ALIGNING BEARINGS
CB	CANTILEVER BEAM
IB	INSTRUMENT BOX
SG	STRAIN-GAGES
TS	TEST SECTION

Figure 4: INSTRUMENT BOX AND CANTILEVER BEAM

during the course of the investigation, each beam being several times more sensitive than the previous one, in order to increase the range of experimentation.

2. Measurement of Frequencies

Each strip chart recorder has the capability of variable, controlled paper speeds. Thus, with chart speed and distance between corresponding points on the trace known, the period of the cyclic signal could be determined. The frequency of oscillation was then simply the reciprocal of the period.

3. Measurement of Acceleration

Acceleration, with the exception of a scale factor, was measured directly from the differential pressure taken from two static pressure taps placed a known distance apart. Neglecting friction losses, the equation of motion yields (Fig. 5),

$$(P_1 - P_3)A_{TS} = ma \tag{4}$$

where m is the mass of fluid. Writing $m = \rho \times A_{TS}$ in (4), one has

$$(P_1 - P_3)A_{TS} = \rho \times A_{TS}\, a \tag{5}$$

or

$$a = \Delta P_{1-3}/\rho X. \tag{6}$$

4. Measurement of Velocity

The dynamic pressure, in the form $\rho U^2/2$, was determined using the differential pressure from the total and static pressure taps 2 and 3, respectively, (Fig. 5), by properly locating the wall pressure tap for a given size cylinder.

Determination of this distance begins with the unsteady Bernoulli equation

$$\frac{DV}{Dt} = \frac{\partial V}{\partial t} + V\frac{\partial V}{\partial s} = -\frac{1}{\rho}\frac{\partial P}{\partial s} \tag{7}$$

which reduces to

$$-\frac{\partial}{\partial s}(P + \rho V^2/2) = \rho\frac{\partial V}{\partial t}. \tag{8}$$

Upon integration, (8) becomes

$$(P + \rho V^2/2)\Big|_1^2 = -\rho\int_1^2 \frac{\partial V}{\partial t}\, ds \tag{9}$$

or

$$P_2 + \rho V_2{}^2/2 - P_1 - \rho V_1{}^2/2 = -\rho\int_1^2 \frac{\partial V}{\partial t}\, ds. \tag{10}$$

It is evident from Figure 5 that $V_2 = 0$ at the stagnation point. Therefore, (10) becomes

$$\Delta P_{1-2} = P_2 - P_1 = -\rho\int_1^2 \frac{\partial V}{\partial t}\, ds + \rho V^2/2. \tag{11}$$

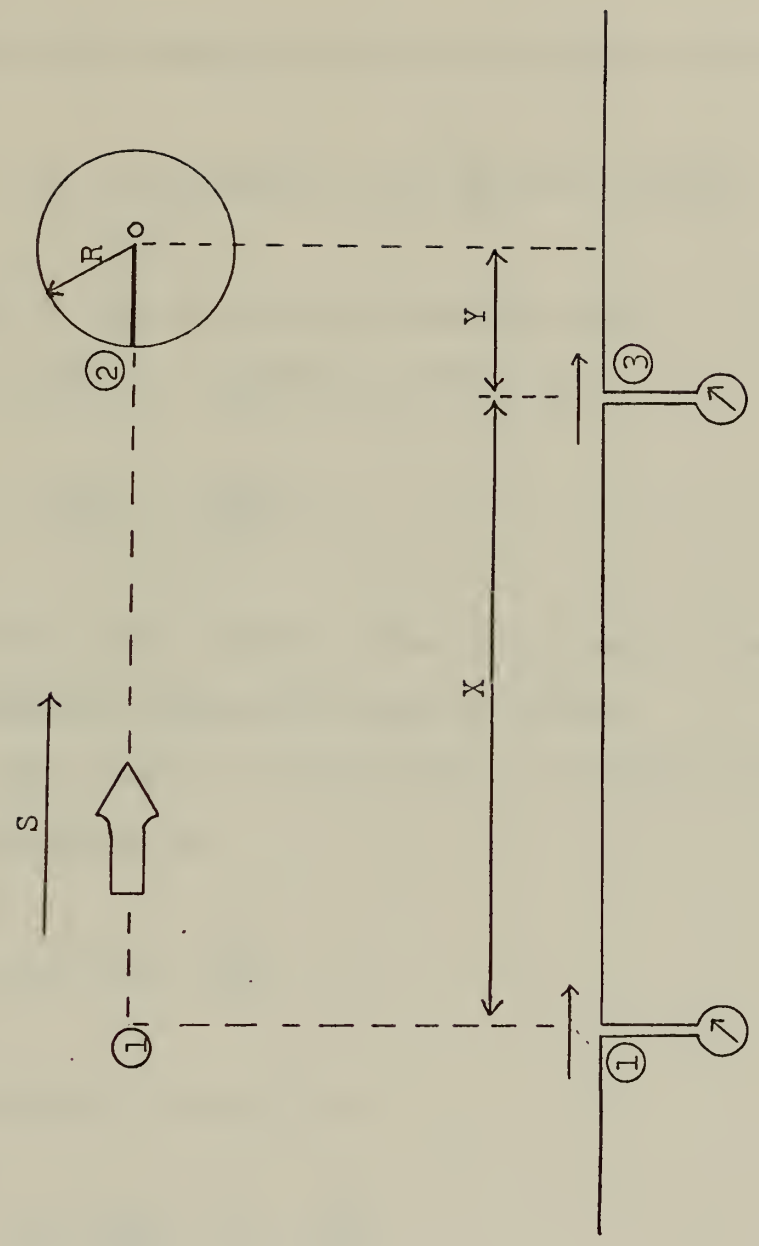

Figure 5: PRESSURE TAP DIAGRAM

Now, from Equation (6)

$$\Delta P_{1-3} = P_3 - P_1 = \rho X \frac{\partial V}{\partial t} \tag{12}$$

and combining these pressure differences yields,

$$P_2 - P_3 = \rho V^2/2 - \rho \int_1^2 \frac{\partial V}{\partial t} ds + \rho X \frac{\partial V}{\partial t} . \tag{13}$$

In order to satisfy the requirement that $P_2 - P_3 = \rho V^2/2$, it is necessary, considering (13), that

$$X \frac{\partial V}{\partial t} = \int_1^2 \frac{\partial V}{\partial t} ds . \tag{14}$$

To evaluate this integral, the variation of V with s along the stagnation streamline must be known.

The complex potential for a cylinder in a uniform stream is given by

$$\Omega = V(Z + \frac{R^2}{Z}) \tag{15}$$

and the complex velocity is

$$W = \frac{d\Omega}{dZ} = V(1 - \frac{R^2}{Z^2}) . \tag{16}$$

But, by definition

$$W = u - iv . \tag{17}$$

Therefore, along the stagnation streamline connecting the points 1 and 2, one has

$$v = 0$$
$$u = V\left(1 - \frac{R^2}{s^2}\right) \tag{18}$$

since Z = -s. Substituting this result into the integral of Eqn. (14) yields

$$\int_1^2 \frac{\partial V}{\partial t}\, ds = \frac{\partial V}{\partial t} \int_1^2 \left(1 - \frac{R^2}{s^2}\right) ds. \tag{19}$$

Carrying out the integration and equating the results with the requirement of (14) yields

$$X \frac{\partial V}{\partial t} = \frac{\partial V}{\partial t}\left(s + \frac{R^2}{s}\right)_1^2 \tag{20}$$

which simplifies to,

$$X = (X + Y) + \frac{R^2}{(X + Y)} - R - \frac{R^2}{R} \tag{21}$$

or

$$Y + \frac{R^2}{(X + Y)} = 2R \tag{22}$$

where (X + Y) is the distance to the point 2 and R is the radius of the cylinder and distance to the point 1.

Since the flow upstream from the cylinder extends to relatively large distances, i.e., as $X \to \infty$, Equation (22) reduces to

$$Y = 2R. \tag{23}$$

Therefore, pressure tap 3 (Fig. 5) must be located one diameter upstream from the center of the cylinder in order to obtain $P_2 - P_3 = \rho U^2/2$.

The length of the test section upstream from the cylinder was sufficiently large to ignore the small influence of the contraction of the flow near the test section on the ambient flow. It is for this reason that X is taken to be effectively infinitely large.

5. Hydrodynamic Tunnel Correction Factors

Steady state tunnel correction factors as discussed in Pope [Ref. 34] account for the fact that the bluff body is not being tested in an infinite medium. There is a blockage-effect correction to the measured velocity, which in turn affects the calculated drag coefficient. In a usable form, this correction factor is given by

$$e = \frac{\pi^2}{12} \left(\frac{d}{h}\right)^2 + \frac{1}{4} \left(\frac{d}{h}\right) C_D \tag{24}$$

where d is the cylinder diameter and h is the height of the tunnel test section. This correction factor is then used to

modify the measured velocity, q, by

$$U = q(1 + e) \tag{25}$$

which then modifies the uncorrected drag coefficient to

$$C_{D_{corr}} = 2F/\rho U^2 \ell d \ . \tag{26}$$

The effect of this correction is to increase the measured velocity and thus to decrease the drag coefficient.

However, with the critical placement of the static pressure tap 3 and its proximity to the test cylinder, another correction must be applied to the measured velocity. From Figure 6, for steady state flows, the ratio of local fluid velocity to the free stream velocity is given by

$$U = \left[\frac{q^2}{1 - 2 \frac{R^2}{r^2} \cos 2\theta + \frac{R^4}{r^4}} \right]^{1/2} \tag{27}$$

For the geometry in this situation, the effect of this correction is to decrease the measured velocity and thus to increase the drag coefficient.

As the effects of (25) and (27) counteract each other in the steady state flow situation, and since no information is available for time-dependent flows, neither correction was applied. This is particularly justified in the present study since the time-dependent drag coefficients were compared

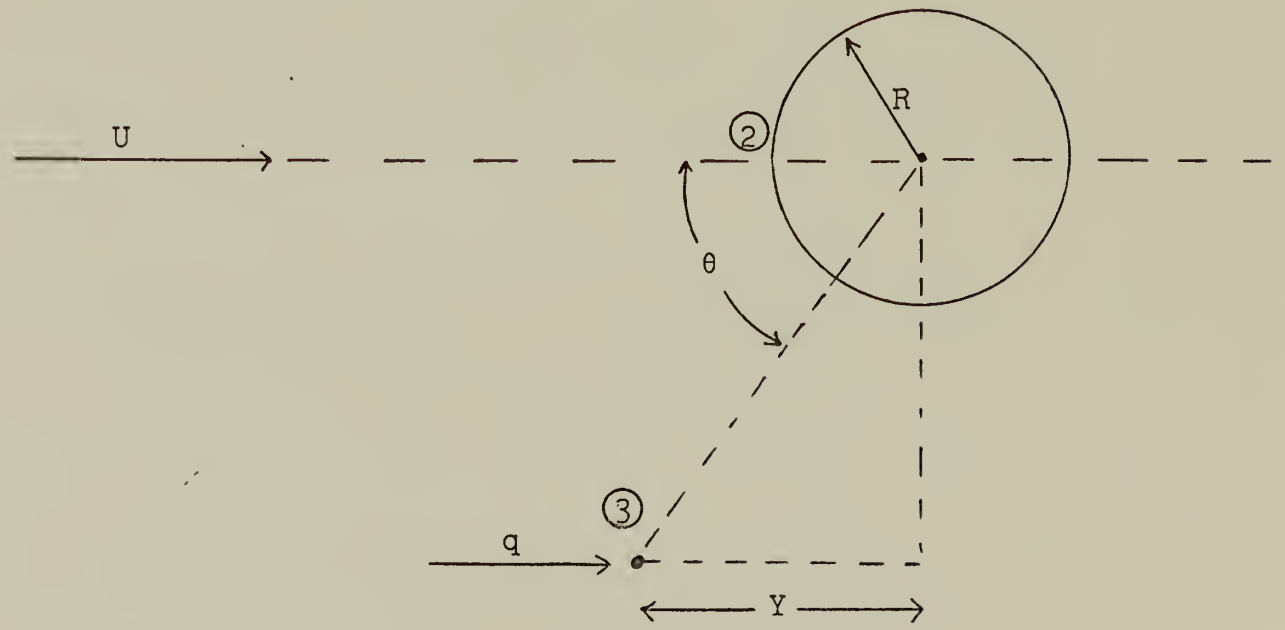

Figure 6: HYDRODYNAMIC CORRECTION FACTOR

with calculated steady drag coefficients, neither being corrected for any hydrodynamic constraints.

III. THEORETICAL CONSIDERATIONS

Assuming that the unidirectional periodic flow in which the test cylinder is immersed is a sinusoidal flow superposed on a steady flow, the instantaneous free stream velocity can be represented as

$$U = \bar{V} + V_A \sin 2\pi ft. \tag{28}$$

Therefore, the instantaneous acceleration becomes

$$a = \frac{dU}{dt} = 2\pi f V_A \cos 2\pi ft \tag{29}$$

and the velocity squared is

$$U^2 = \bar{V}^2 + 2\bar{V}V_A \sin 2\pi ft + V_A^2 \sin^2 2\pi ft. \tag{30}$$

Now, in dealing with the total force acting on the cylinder in time-dependent flows, it has been most advantageous to consider it as composed of a drag force and an inertial force, such as

$$F = F_D + F_I. \tag{31}$$

Then using the concept of the normalized drag and inertia resistance coefficients, C_D and C_M, respectively, the total

force can be represented as

$$F = C_D \tfrac{1}{2} A \rho U^2 + C_M \ell \rho A_o \frac{dU}{dt} \tag{32}$$

where A is the effective cylinder flow-blockage area, A_o is the cylinder cross-sectional area, ℓ is the cylinder length, and ρ the fluid density. Upon substitution of (29) and (30) into (32), one obtains,

$$\begin{aligned} F = {} & C_D[\tfrac{1}{2} A \rho \bar{V}^2 + A \rho \bar{V} V_A \sin 2\pi ft + \tfrac{1}{2} A \rho V_A^2 \sin^2 2\pi ft] \\ & + C_M[\rho \ell A_o 2\pi f V_A \cos 2\pi ft]. \end{aligned} \tag{33}$$

However, the results of the works previously cited indicate that a two parameter total-force equation does not seem to be capable of providing sufficient generality to cover the conditions encountered in arbitrary time-dependent flows. Also, the past history of the flow must be considered along with the velocity, rate of change of velocity, and Reynolds number. Therefore, defining $C_D(0)$ as the steady state coefficient of drag which occurs at time t = 0 when $U = \bar{V}$, and assuming that a normalized frequency parameter $\lambda = fd/\bar{V}$ provides the necessary correlation between the resistance coefficients and the aforementioned flow parameters, the total force can be written as

$$F = C_D(0)\tfrac{1}{2}A\rho\bar{V}^2$$

$$+ C_D(\lambda)[\bar{V}V_A A\rho \sin 2\pi ft + \tfrac{1}{2}A\rho V_A^2 \sin^2 2\pi ft] \quad (34)$$

$$+ C_M(\lambda)[A_o \rho \ell 2\pi f V_A \cos 2\pi ft].$$

The coefficients $C_D(0)$, $C_D(\lambda)$, and $C_M(\lambda)$ are determined experimentally. It is obvious that the validity of the foregoing analysis depends upon the existance of a correlation between the said coefficients and the normalized oscillation parameter, λ, for various values of Reynolds number, λ, and $V_A/\bar{V}$.

IV. EVALUATION AND PRESENTATION OF DATA

A. RAW DATA

As cited earlier, the differential pressure directly provides the velocity in squared form. Figure 7 shows a theoretical curve of $U^2 = (\overline{V} + V_A \sin 2\pi ft)^2$ with $\overline{V} = 1.5$ and $V_A = 0.5$. The distances labeled p and r occur at $t = T/4$ and $t = 3T/4$, respectively. With these distances known, $\overline{V}$, V_A, and U^2 at time $t = T/8$ can be calculated as follows. Writing at the specific times,

$$t = T/4 \qquad U^2 = (\overline{V} + V_A)^2 = p \tag{35}$$

$$t = 3T/4 \qquad U^2 = (\overline{V} - V_A)^2 = r \tag{36}$$

$$t = T/8 \qquad U^2 = (\overline{V} + V_A \sqrt{2}/2)^2 \tag{37}$$

one has

$$\overline{V} + V_A = \sqrt{p} \tag{38}$$

and

$$\overline{V} - V_A = \sqrt{r} \tag{39}$$

which yields

$$\overline{V} = (\sqrt{p} + \sqrt{r})/2. \tag{40}$$

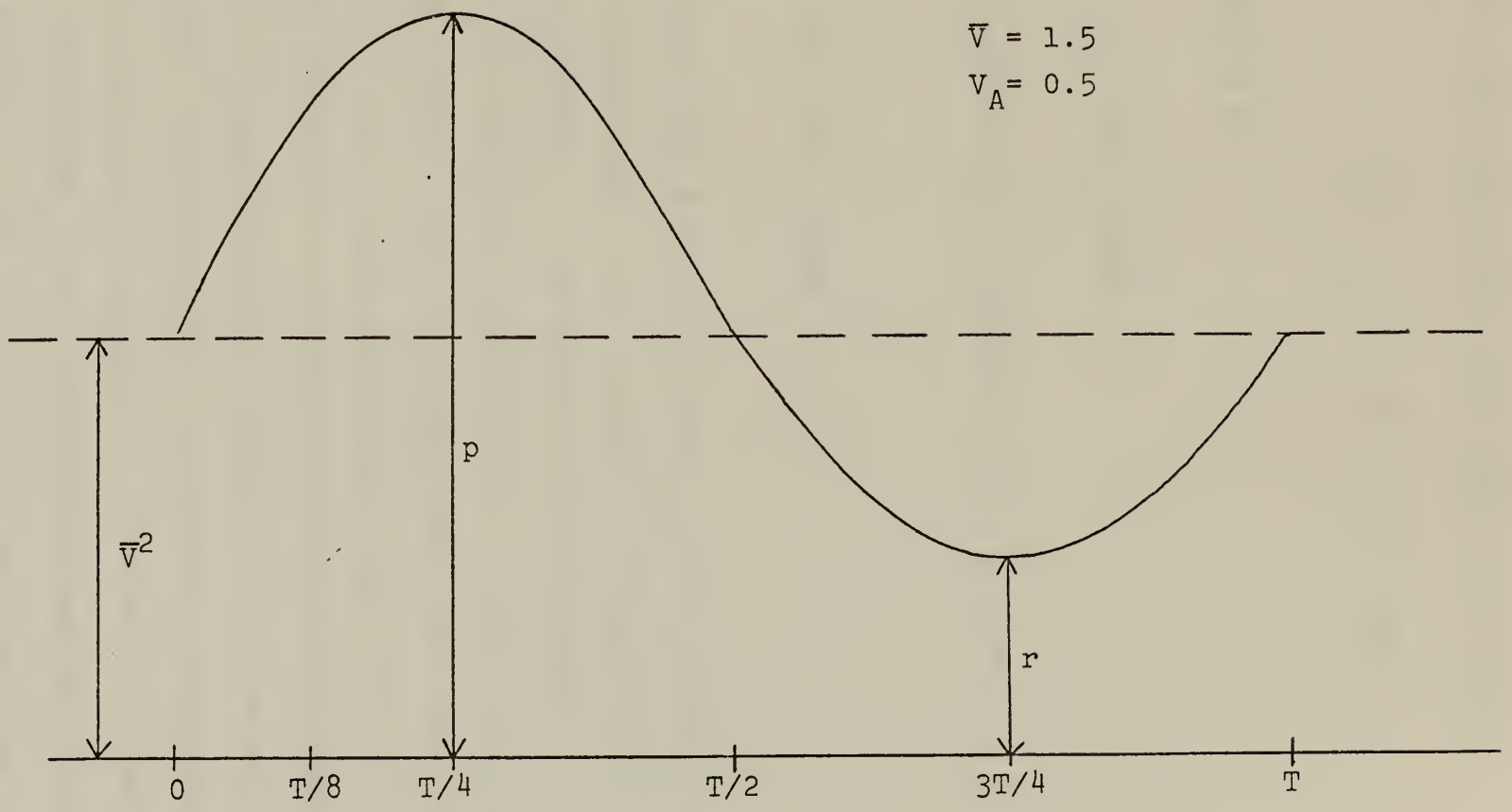

Figure 7: THEORETICAL SHAPE OF THE SQUARED-VELOCITY

Now, upon subtracting (36) from (35), one obtains

$$p - r = (\bar{V} + V_A)^2 - (\bar{V} - V_A)^2 = 4\bar{V}V_A \qquad (41)$$

which reduces to

$$V_A = (p - r)/4\bar{V}. \qquad (42)$$

Also upon expansion of equation (37), at time t = T/8, one has

$$U^2 = \bar{V}^2 + \sqrt{2}\bar{V}V_A + \tfrac{1}{2}V_A^2 \qquad (43)$$

Figures 8 and 9 display copies of strip chart recordings of typical data sets for low and high frequencies of oscillation, respectively. The upper traces represent $\Delta P_{2-3} = \rho U^2/2$ while the lower traces indicate the instantaneous total force. Due to the fact that the torque curve of a butterfly valve is not symmetrical about 45°, nor the discharge coefficient (and thus the head loss) symmetrical about 90° in unidirectional flow [Ref. 33], the velocity curve is not a pure sinusoid. Therefore, the following procedure was used in reducing the raw data to usable form:

1. The period, T, was measured between any two corresponding points on the curve. Thus T was the true period of the repetitive signal.

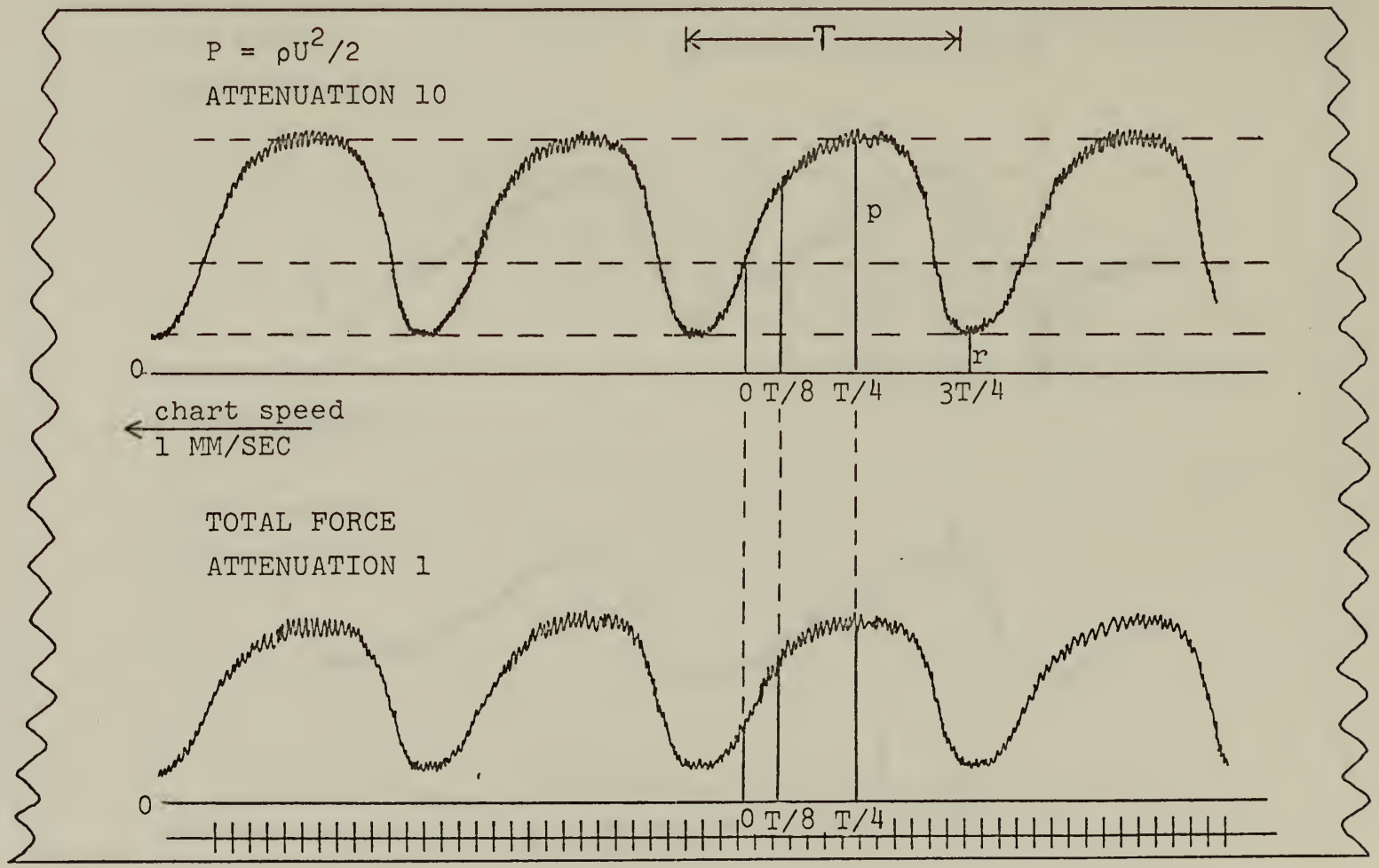

Figure 8: TYPICAL CHART TRACE AT LOW FREQUENCY OF OSCILLATION

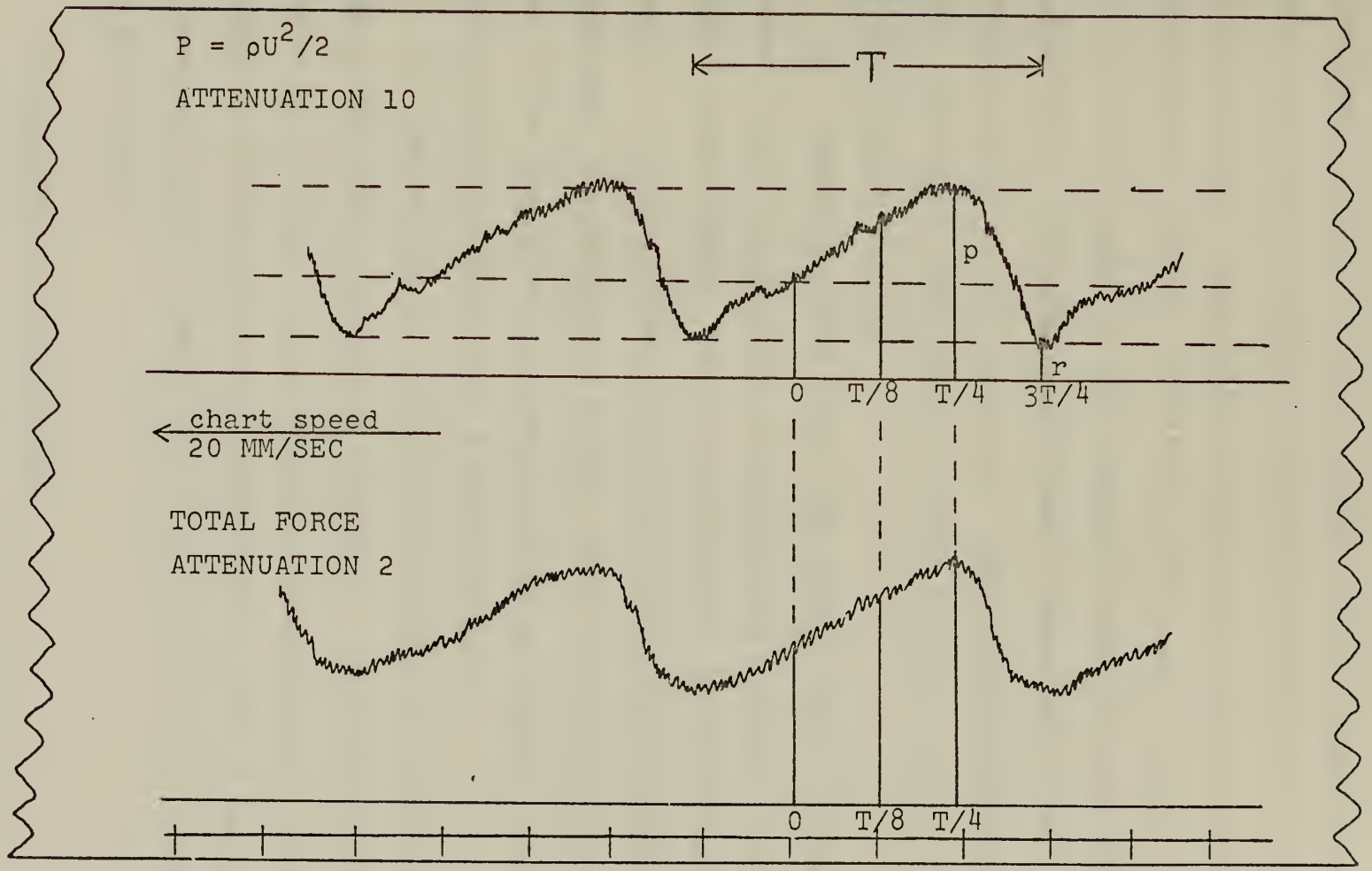

Figure 9: TYPICAL CHART TRACE AT HIGH FREQUENCY OF OSCILLATION

2. The distances p and r were measured to the highest and lowest points on the pressure curve, respectively. The occurrance of these points were labeled T/4 and 3T/4 irrespective of their distance on the time axis since the minimum and maximum velocities will occur at these times.

3. The height at the squared-velocity curve at times t = 0 and t = T/8 were calculated from p and r as if the velocity were a true sinusoid. The corresponding points on the curve were then found at these heights, and the base line marked 0 and T/8.

4. Vertical lines were then drawn from the pressure curve to the force curve at the places marked 0, T/8, and T/4, and the height of the force curve tabulated at these points. Since the two traces are made simultaneously and represent instantaneous values, these quantities then give the forces which would have occurred at times 0, T/8, and T/4 had the velocity been a true sinusoid.

5. The values of velocity and force were then calculated from the calibration equations. Reynolds number based on the mean velocity was also calculated. For this purpose, an average water temperature of 70° F was assumed for evaluating the density and viscosity of the tap water in the tunnel.

B. EVALUATION OF COEFFICIENTS

As detailed in Part III, the total force acting on the cylinder is assumed to take the form

$$F = C_D(0)[\tfrac{1}{2}A\rho\bar{V}^2]$$

$$+ C_D(\lambda)[\bar{V}V_A A\rho \sin 2\pi ft + \tfrac{1}{2}A\rho V_A{}^2 \sin^2 2\pi ft] \quad (44)$$

$$+ C_M(\lambda)[2\pi A_o \rho \ell f V_A \cos 2\pi ft]$$

After the reduction of the raw data, at times t = 0, t = T/8, and t = T/4 all the variables with the exception of $C_D(0)$, $C_D(\lambda)$, and $C_M(\lambda)$ are known. However, a system of three equations for the three unknowns can be developed. Re-writing (44) as

$$F = C_D(0)K_1$$

$$+ C_D(\lambda)[K_2 \sin 2\pi ft + K_3 \sin^2 2\pi ft] \quad (45)$$

$$+ C_M(\lambda)[K_4 \cos 2\pi ft]$$

and evaluating (45) at times 0, T/4, and T/8 results in

$$t = 0 \qquad F = C_D(0)K_1 + C_M(\lambda)K_4 \quad (46)$$

$$t = T/8 \qquad F = C_D(0)K_1 + C_D(\lambda)[K_2 \sqrt{2}/2 + K_3 \tfrac{1}{2}] \quad (47)$$

$$+ C_M(\lambda)K_4 \sqrt{2}/2$$

$$t = T/4 \qquad F = C_D(0)K_1 + C_D(\lambda)[K_2 + K_3] \quad (48)$$

These three equations can be solved simultaneously for $C_D(0)$, $C_D(\lambda)$, and $C_M(\lambda)$.

However, in the range of experimentation of this study, the ratio of inertia forces to that of the drag forces was << 1. This fact led to problems of instability in the matrix used to solve for the inertia coefficient. For this reason, $C_M(\lambda)$ was fixed at a chosen value, and the values of $C_D(0)$ and $C_D(\lambda)$ were solved using the instantaneous data at times t = 0 and t = T/4. The two resulting equations were

$$t = 0 \qquad C_D(0) = \frac{F - C_M K_4}{K_1} \tag{49}$$

and

$$t = T/4 \qquad C_D(\lambda) = \frac{F - C_D(0)K_1}{(K_2 + K_3)} \tag{50}$$

The coefficients $C_D(0)$ and $C_D(\lambda)$ were calculated from (49) and (50) by using two different values for $C_M(\lambda)$. First, a theoretical value of $C_M(\lambda) = 2$ for unseparated potential flow and second, a semi-theoretical and semi-experimental value of $C_M(\lambda) = 1.5$ [Refs. 25,35] were used. The resulting values of $C_D(0)$ and $C_D(\lambda)$ were essentially unchanged. The difference between $C_D(0)$ with $C_M(\lambda) = 2$ and $C_D(0)$ with $C_M(\lambda) = 1.5$ was negligible to the second decimal. This also held true for $C_D(\lambda)$.

C. NORMALIZED PLOTS

The non-dimensional drag coefficient $C_D(0)$ is presented in Figure 10 as a function of the Reynolds number based on average velocities.

The coefficients $C_D(0)$, $C_D(\lambda)$, and $C_M(\lambda)$ are then presented as functions of the normalized frequency parameter, λ (Figs. 11-15).

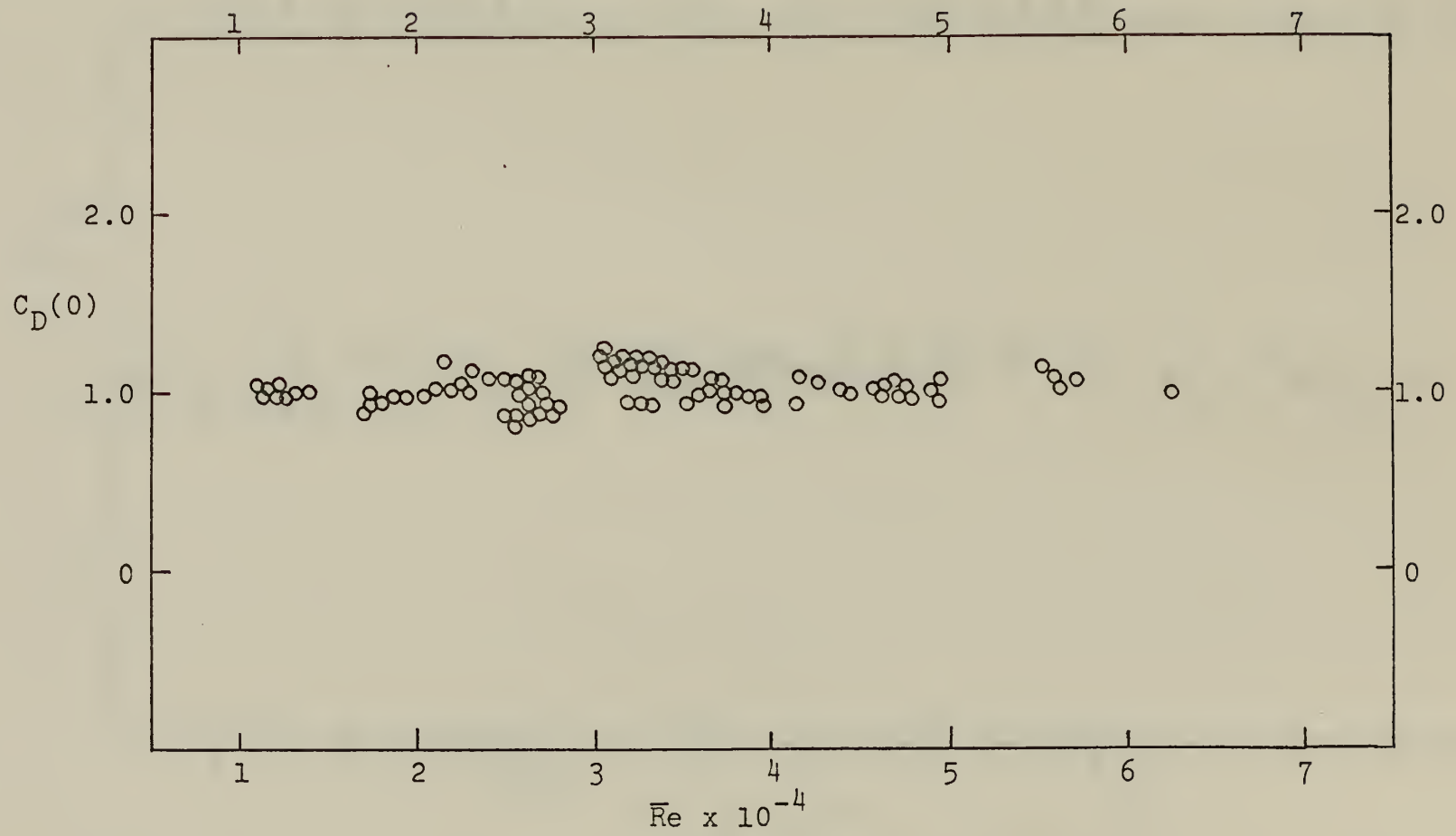

Figure 10: $C_D(0)$ VERSUS REYNOLDS NUMBER

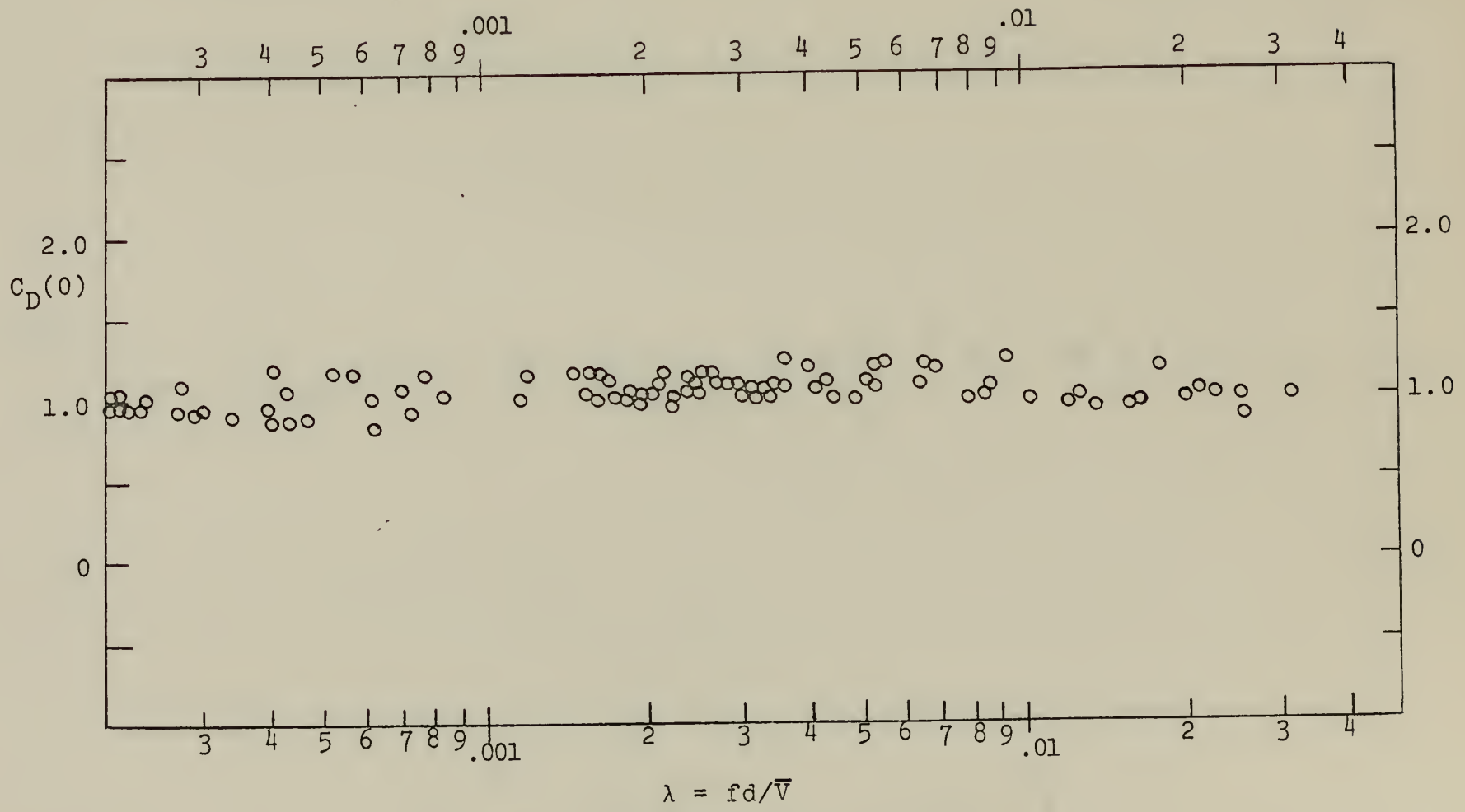

Figure 11: $C_D(0)$ FOR $.0002 < \lambda < .05$

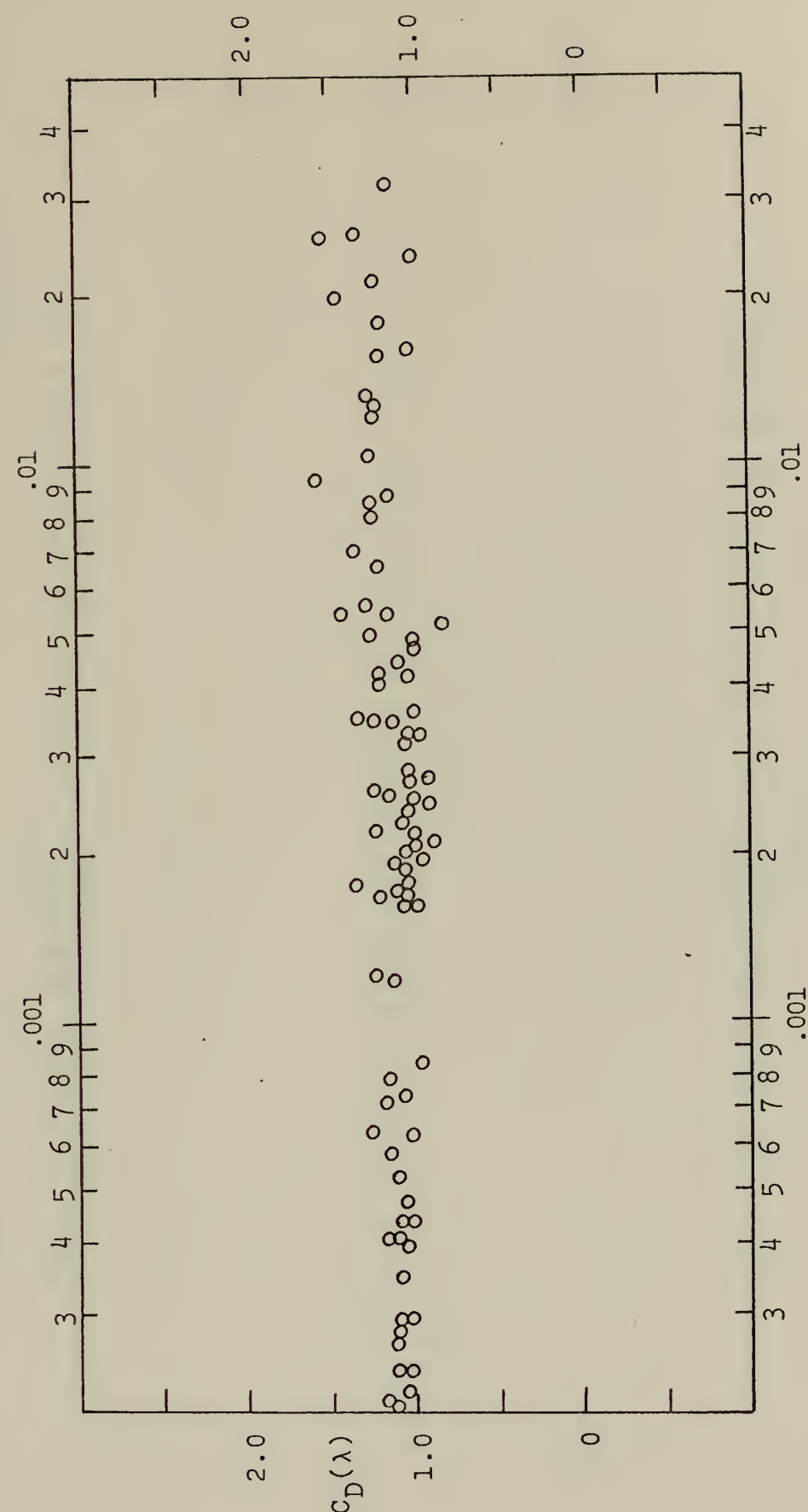

Figure 12: $C_D(\lambda)$ FOR $.0002 < \lambda < .05$

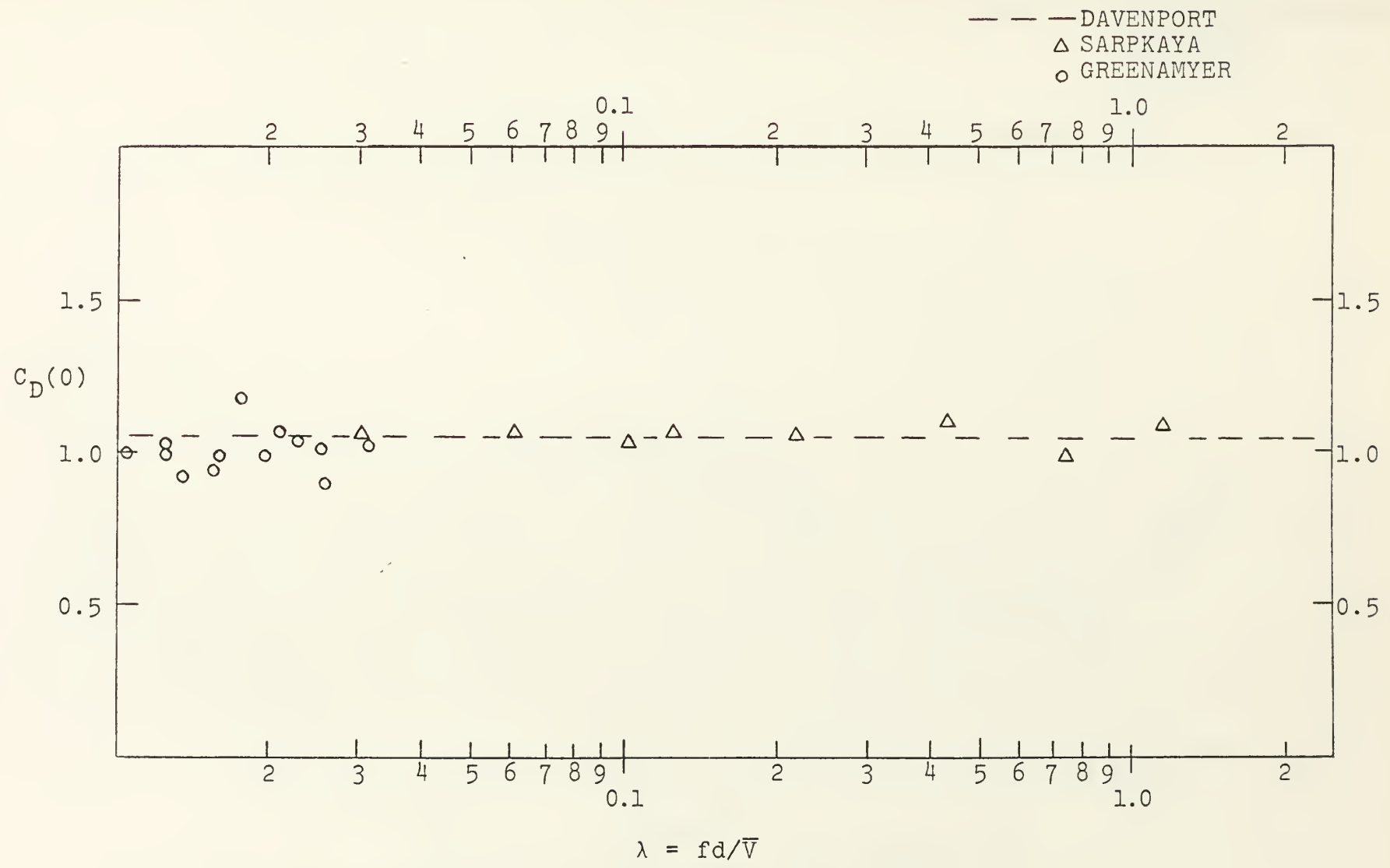

Figure 13: $C_D(0)$ FOR $.01 < \lambda < 2.5$

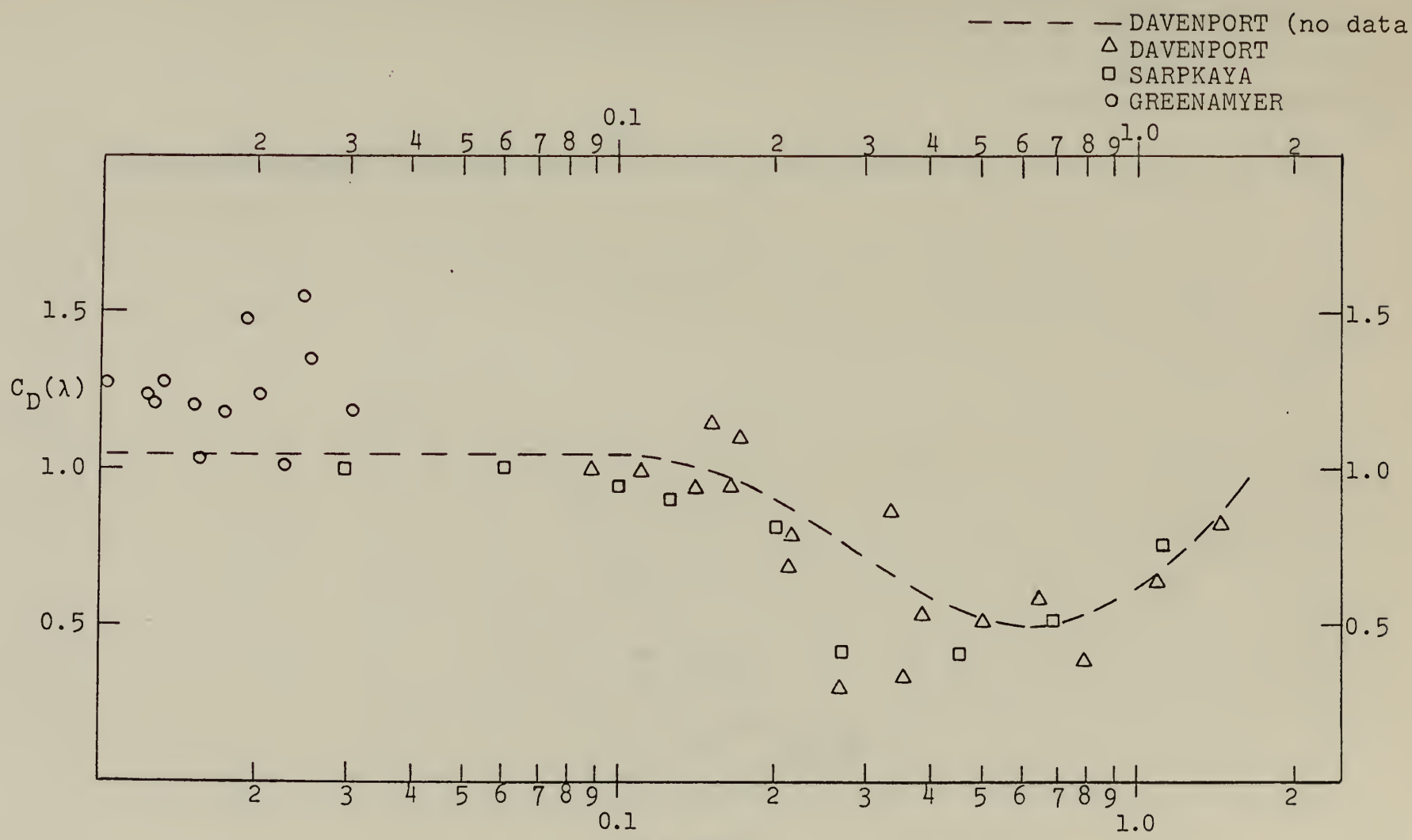

Figure 14: $C_D(\lambda)$ FOR $.01 < \lambda < 2.5$

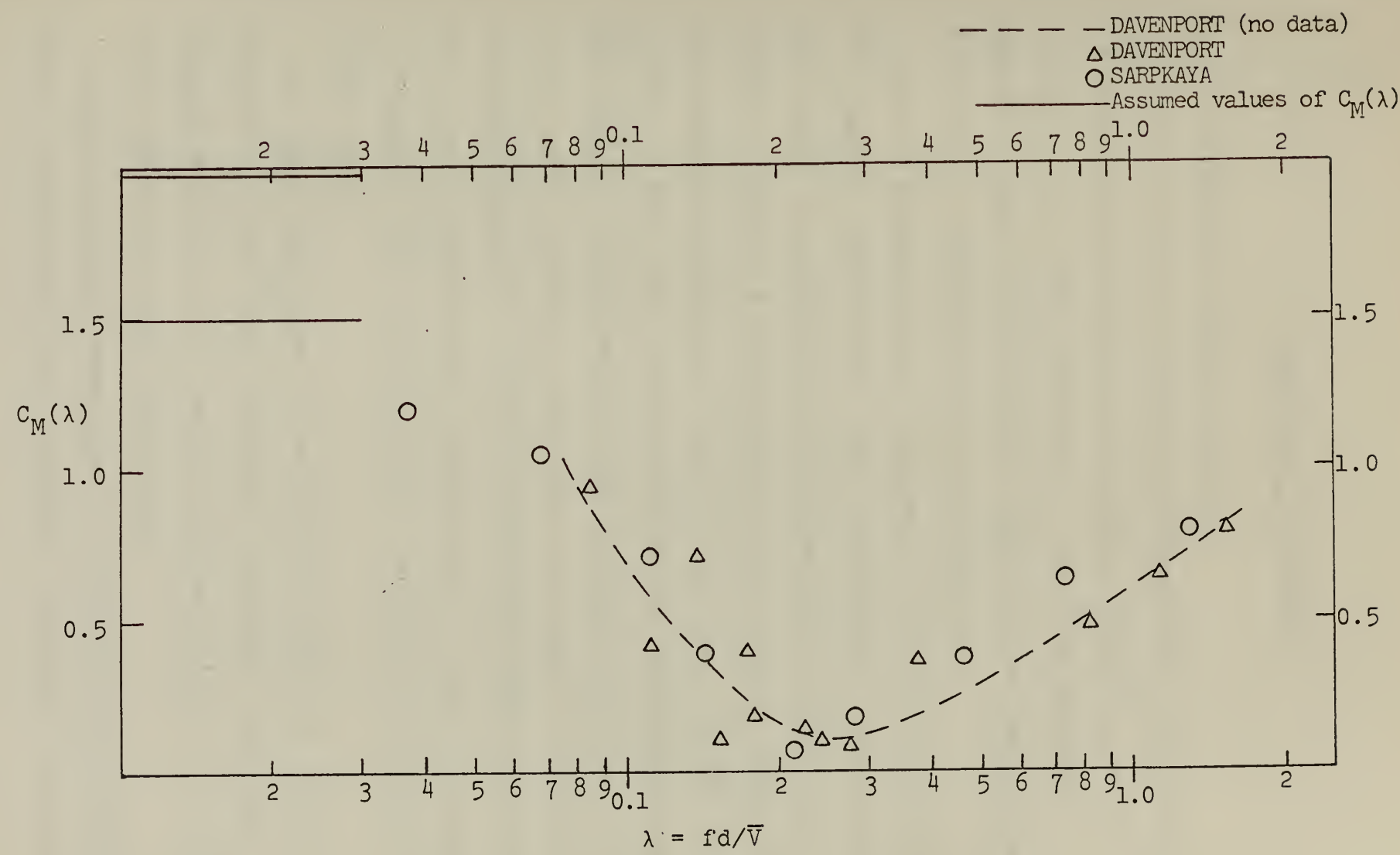

Figure 15: $C_M(\lambda)$ FOR $.01 < \lambda < 2.5$

V. DISCUSSION OF RESULTS

A. UNIDIRECTIONAL PERIODIC MOTION

Although the flow remained unidirectional and periodic, its oscillatory motion was not quite sinusoidal, as discussed in Section IV. This aberration in the flow appeared to manifest itself differently for high and low frequencies of oscillation, irrespective of the value of λ.

At low frequencies of oscillation (Fig. 8) the curve of $\rho U^2/2$ appears symmetrical about the vertical with the absolute values of acceleration and deceleration about equal. However, there is a long period in the cycle at which the valve appears to have no effect on the flow. At the highest portion of the curve the valve is in the horizontal position with respect to the conduit axis (minimum head loss), while at the lowest portion of the curve the valve is vertical (maximum head loss). It is thus apparent that the available head is not significantly changed when the valve is about $\pm$ 30 degrees from the horizontal, causing a flat portion in the curve.

At high frequencies of oscillation (Fig. 9), this "null portion" of valve travel creates a pressure curve which is unsymmetrical about the vertical characterized by a small acceleration and rapid deceleration.

Several attempts were made to alleviate this problem. First, a baffle plate was installed upstream of the valve

to decrease $\bar{V}$. At this time vertical ridges extending downstream were attached around the holes in the baffle in order to decrease the magnitude of the deceleration. Second, small vertical plates were attached perpendicular to the valve faces so that the valve might affect the head loss in the near horizontal position. Finally, two plates were attached perpendicular to the valve faces with the same diameter as the valve itself to form a four-bladed butterfly valve. Unfortunately, time did not permit manufacturing the plates to the same width or contour as the existing valve.

It is for this reason that only those portions of a cycle which most nearly exhibited a sinusoidal velocity variation were used in evaluating the various coefficients. A butterfly valve system consisting of several plates is anticipated to alleviate this problem and yield a fairly sinusoidal oscillation in velocity over the entire cycle.

B. EXTENSION AND COMPARISON OF DATA WITH THOSE OBTAINED BY OTHERS

The data obtained herein are presented together with those obtained by Davenport [Ref. 36] at the University of Bristol and by Sarpkaya [Ref. 31] at the Aerodynamische Versuchsanstalt, Göttingen, using a circular cylinder of 1 inch diameter in an oscillating wind tunnel within the range of Reynolds numbers from 5000 to 90,000.

First, it is apparent that the data of Davenport and Sarpkaya constitute extensions of the present data to higher values of the frequency parameter, λ.

Second, it is clear that all of the data correlate fairly well with λ over a large range of λ and Reynolds numbers regardless of whether it is obtained with air or water in a small or large tunnel.

Third, it is evident that the effects of the free-stream oscillations on $C_M(\lambda)$ become significant only when the frequency of oscillation approaches the natural vortex-shedding frequency, i.e. when λ approaches the Strouhal number of about 0.2. Although a theoretical explanation of the decrease of $C_M(\lambda)$ as $\lambda \to St$ is beyond the scope of the present study, it is not too much of a conjecture to state that the formation, growth, and motion of the vortices are significantly altered by the oscillations when the shedding frequency is in the neighborhood of the oscillatory frequency of the free stream. When the period of oscillation is several orders of magnitude larger than the period of vortex shedding, the flow behaves essentially as a juxtaposition of instantaneous quasi-steady states and the total resistance can be represented accurately by the coefficients $C_D(0)$ and $C_D(\lambda)$.

Finally, it is evident that $C_D(\lambda)$ decreases sharply in the range of $fd/\overline{V}$ from 0.25 and 0.5. The reasons for this are as follows. It is a well-known fact that the drag acting on a cylinder undergoes oscillations with a frequency twice the frequency of vortex shedding. In other words, as the lift force changes its direction, up or down, the drag force oscillates with an amplitude of ΔC_D about a mean value

of C_D. Denoting the oscillation frequency of drag with f_D, we then have $f_D d/\bar{V} \simeq 0.44$. The same parameter for the lift oscillations is $f_\ell d/\bar{V} \simeq 0.22$ within the range of Reynolds numbers studied. Thus the data presented in Fig. 14 show that $C_D(\lambda)$ is, and should be, affected in the range of $fd/\bar{V}$ from 0.25 to 0.5, i.e. as the drag-oscillation frequency nearly synchronizes with the free-stream oscillation frequency. Only a complete analytical investigation, if at all possible, can explain as to why $C_D(\lambda)$ should decrease.

VI. CONCLUSIONS

The conclusions which can be drawn from this study are:

1. The frequency parameter λ correlates fairly well the data obtained by various investigators regarding the resistance coefficients.

2. In the range of $0 < \lambda < 0.05$, the resistance coefficients are not materially affected by the free-stream oscillations. This range has not been previously investigated. All or most of the previous studies have dealt with oscillations with a zero mean velocity, i.e. with $\lambda \to \infty$.

3. The drag and inertia coefficients which are functions of the frequency parameter λ are significantly reduced in the range where the free stream oscillations nearly coincide with the flow induced oscillations of lift and drag.

4. The reasons leading to the decrease in $C_D(\lambda)$ and $C_M(\lambda)$ in the vicinity of $\lambda = 0.4$ and $\lambda = 0.2$ respectively, can be clarified only by a combination of additional theoretical and experimental investigations where the full Navier-Stokes equations are solved for an oscillatory flow about a circular cylinder and where the characteristics of flow in the near-wake of the cylinder are measured.

VII. RECOMMENDATIONS FOR FURTHER STUDIES

The following are recommendations for further studies:

1. Improve the butterfly valve system so that nearly sinusoidal oscillations may be obtained in the range of $0 < \lambda < 2.0$.

2. Undertake a study of the solution of the Navier-Stokes equations via finite-difference or finite-element methods for the range of λ values cited above.

3. Carry out experiments with flat plates and other shapes of bodies to ascertain the universality of the parameter λ.

LIST OF REFERENCES

1. Sarpkaya, T., "On Time-Dependent Flows of Incompressible Fluids," Developments in Mechanics, Midwestern Mechanics Conference, vol. 5, 1969. pp:985-1001.

2. Stewartson, K., "The Theory of Unsteady Laminar Boundary Layers," Advances in Applied Mechanics, Ed. H. L. Dryden et alli., Academic Press, N.Y., vol. VI, 1960, pp: 1-37.

3. Stuart, J.T., "Unsteady Boundary Layers," Laminar Boundary Layers, Ed. L. Rosenhead, Oxford Univ. Press, Oxford, 1963, pp: 349-406.

4. Rott, N., "Theory of Time-Dependent Flows," Theory of Laminar Flows, Ed. F. K. Moore, Princeton Univ. Press, Princeton, 1964, pp: 395-438.

5. Stelson, T.E. and Mavis, F.T., "Virtual Mass and Acceleration in Fluids," Trans. ASCE, Paper No. 2870, 1955, pp: 518-530.

6. Sarpkaya, T., "Added Mass of Lenses and Parallel Plates," Jour. of Engineering Mechs. Div., ASCE, vol. 86, No. EM3, June 1960, pp: 141-152.

7. Mavis, T., "Virtual Mass of Plates and Discs in Water," ASCE Proc. Paper No. 7593, Oct. 1970, (See also discussion by C.J. Garrison in ASCE Proc. Paper No. 8012, April 1971, pp: 631-635).

8. Goldschmidt, V.W. and Protos, A., "Added Mass of Equilateral-Triangular Cylinders," Jour. of Engineering Mechs. Div. ASCE, EM6, Dec. 1968, pp: 1539-1545.

9. Hamilton, W.S. & Lindell, J.E., "Fluid Force Analysis and Accelerating Sphere Tests", Jour. of the Hydraulics Div. ASCE, HY6, June 1971, pp: 805-817.

10. Lord Rayleigh, "On The Motion of Solid Bodies Through Viscous Fluid," Phil. Mag. Series 6, Vol. 21, 1911, p. 697.

11. Odar, F. & Hamilton, W.S., "Forces on a Sphere Accelerating in a Viscous Fluid," Jour. of Fluid Mechs., Vol. 18, part 2, 1964, pp: 302-314.

12. Laird, A.D.K., "Water Forces on a Flexible Oscillating Cylinder," Jour. of Waterways and Harbors Div. ASCE, WW3, Paper No. 3234, 1963, pp: 125-137.

13. Laird, A.D.K., Johnson, C.A. & Walker, R.W., "Water Eddy Forces on Oscillating Cylinders," Trans. ASCE, Vol. 127, 1962, pp: 335-351.

14. Hamann, F. & Dalton, C., "The Forces on a Cylinder Oscillating Sinusoidally in Water," Jour. Engrg. Ind., Trans. ASME, Vol. 93B, 1971, pp: 1197-1203.

15. Roos, F.W. & Willmarth, W.W., "Some Experimental Results on Sphere and Disk Drag," AIAA, Vol. 9, No. 2, Feb. 1971, pp: 285-291.

16. Morison, J.R., O'Brien, M.P., Johnson, J.W. & Schaaf, S.A., "The Force Exerted by Surface Waves on Piles," Petroleum Trans., AIME, Vol. 189, 1950, pp: 149-157.

17. Keulegan, G.H. & Carpenter, L.H., "Forces on Cylinders and Plates in an Oscillating Fluid," Journal of Research, NBS, Vol. 60, 1958, pp: 423-440.

18. Jen, Y., "Laboratory Study of Inertia Forces on a Pile," Jour. of Waterways and Harbors, Proc. ASCE, Vol. 94, WW1, 1968, pp: 59-76.

19. McNown, J.S., "Drag in Unsteady Flow," Proc. 9th International Congress of Applied Mechs., Vol. 3, Brussels, 1957.

20. McNown, J.S. and Keulegan, G.H., "Vortex Formation and Resistance in Periodic Motion," Proc. ASCE, vol. 85, No. EM1, 1959.

21. Brater, E.F., McNown, J.S., and Stair, L.D., "Wave Forces on Submerged Structures," Trans. ASCE, Paper No. 3182, 1958, pp: 661-696.

22. Iverson, H.W. and Balent, R., "A Correlating Modulus for Fluid Resistance in Accelerated Motion," Jour. of Applied Physics, vol. 22, 1951, p. 325.

23. Keim, S.R., "Fluid Resistance to Cylinders in Accelerated Motion," Proc. ASCE, Jour. of Hydraulics Div., vol. 82, Dec. 1956.

24. Laird, A.D.K., Johnson, C.A., and Walker, R.W., "Water Forces on Accelerated Cylinders," Jour. of Waterways and Harbours Div., ASCE, WW1, 1959, pp: 99-119.

25. Sarpkaya, T. and Garrison, C.J., "Vortex Formation and Resistance in Unsteady Flow," Jour. of Applied Mechs., vol. 30, Trans. ASME, vol. 85E, 1963, pp: 16-24.

26. Bishop, R.E.D. and Hassan, A.Y., "The Lift and Drag Forces on a Circular Cylinder Oscillating in a Flowing Fluid," Proc. of the Royal Society, London, Ser. A., vol. 272, 1964.

27. Chen, C.F. and Ballengee, D.B., "Vortex Shedding from Circular Cylinders in an Oscillating Freestream," AIAA Jour., vol. 9, No. 2, Feb. 1971, pp: 340-342.

28. Hatfield, H.M. and Morkovin, M.V., "Effect of an Oscillating Free Stream on the Unsteady Pressure on a Circular Cylinder," ASME Paper No. 72-WA/FE-12, 1972.

29. Mercier, J.A., A discussion of (Blevins, R., "Vortex Induced Vibration of Circular Cylindrical Structures," ASME Paper No. 72 - WA/FE - 39, 1972.), presented at the 1972 Winter Annual Meeting of ASME, N.Y., 1972.

30. Davenport, A.G., "The Application of Statistical Concepts to the Wind Loading of Structures," The Institute of Civil Engineers, vol. 19, 1961, pp: 449-472.

31. Sarpkaya, T., unpublished data obtained by him at Aerodynamische Versuchsanstalt, Göttingen, 1972.

32. Sarpkaya, T., "Torque and Cavitation Characteristics of Butterfly Valves," Jour. of Applied Mechs., vol. 28, No. 4, Dec. 1961, pp: 511-518.

33. Guins, V.G., "Flow Characteristics of Butterfly and Spherical Valves," Jour. of Hydraulics Div. ASCE, vol. 94, No. HY3, May 1968, pp: 675-690.

34. Pope, A., Wind Tunnel Testing, John Wiley and Sons, Inc., N.Y., 1954, pp: 277-280.

35. Sarpkaya, T., "Lift, Drag, and Added-Mass Coefficients for a Circular Cylinder Immersed in a Time-Dependent Flow," Jour. of Applied Mechs., vol. 30, No. 1, March 1963, pp: 13-15.

36. Davenport, A.G., "A Statistical Approach to the Wind Loading of the Tall Mast and Suspension Bridge," Ph.D. Thesis, University of Bristol, Dept. of Civil Engineering, 1971.

INITIAL DISTRIBUTION LIST

		No. Copies
1.	Defense Documentation Center Cameron Station Alexandria, Virginia 22314	2
2.	Library, Code 0212 Naval Postgraduate School Monterey, California 93940	2
3.	Mechanical Engineering Department Library, Code 59 Naval Postgraduate School Monterey, California 93940	1
4.	Professor T. Sarpkaya, Code 59SL Department of Mechanical Engineering Naval Postgraduate School Monterey, California 93940	1
5.	Lieutenant Richard D. Greenamyer, USN SMC 1332 Naval Postgraduate School Monterey, California 93940	1

Security Classification

DOCUMENT CONTROL DATA - R & D

(Security classification of title, body of abstract and indexing annotation must be entered when the overall report is classified)

1. ORIGINATING ACTIVITY (Corporate author)

Naval Postgraduate School
Monterey, California 93940

2a. REPORT SECURITY CLASSIFICATION

Unclassified

2b. GROUP

3. REPORT TITLE

Unidirectional Periodic Flow About Circular Cylinders

4. DESCRIPTIVE NOTES (Type of report and, inclusive dates)

Master's Thesis; June 1973

5. AUTHOR(S) (First name, middle initial, last name)

Richard Doyle Greenamyer

6. REPORT DATE	7a. TOTAL NO. OF PAGES	7b. NO. OF REFS
June 1973	61	36

8a. CONTRACT OR GRANT NO.	9a. ORIGINATOR'S REPORT NUMBER(S)
b. PROJECT NO.	
c.	9b. OTHER REPORT NO(S) (Any other numbers that may be assigned this report)
d.	

10. DISTRIBUTION STATEMENT

Approved for public release; distribution unlimited.

11. SUPPLEMENTARY NOTES	12. SPONSORING MILITARY ACTIVITY
	Naval Postgraduate School Monterey, California 93940

13. ABSTRACT

The instantaneous force acting on a circular cylinder immersed in a unidirectional periodic flow characterized by $U = \overline{V} + V_A \sin 2\pi ft$ was investigated. The total force was divided into three components consisting of a steady-state drag; an oscillating drag which is a function of the frequency parameter $\lambda = fd/\overline{V}$; and an inertial force which is also a function of the frequency parameter. The three resistance coefficients associated with the force components, $C_D(0)$, $C_D(\lambda)$, and $C_M(\lambda)$ were calculated.

It was found that the resistance coefficients are not materially affected by the free-stream oscillations whenever the frequency of the oscillation is lower than the natural frequency of the vortex shedding. However, when λ approaches the Strouhal frequency of vortex shedding, the inertia coefficient C_M is significantly reduced, and likewise when λ approaches the value of twice the Strouhal number, $C_D(\lambda)$ is markedly reduced. In regions below this range, the inertial force becomes negligible and the total resistance could be represented accurately by the coefficients $C_D(0)$ and $C_D(\lambda)$ with C_M fixed at its theoretical unseparated-flow value, 2.0.

DD FORM 1 NOV 68 1473 (PAGE 1)

S/N 0101-807-6811

Security Classification

A-31408

KEY WORDS	LINK A		LINK B		LINK C	
	ROLE	WT	ROLE	WT	ROLE	WT
Periodic Flow						
Unidirectional Periodic Flow						
Time Dependent Flow						
Drag						
Resistance Coefficients						
Vortex Shedding						